Electronic Supplementary Material (ESI) for Nanoscale.

Supporting Information

Mixed Multilayered Vertical Heterostructures Utilizing Strained Monolayer WS_2

*Yuewen Sheng[1], Wenshuo Xu[1], Xiaochen Wang[1], Zhengyu He[1], Youmin Rong[1], Jamie H. Warner[1]**

[1]Department of Materials, University of Oxford, Parks Road, Oxford, OX1 3PH, United Kingdom

*Jamie.warner@materials.ox.ac.uk;

S1. AFM Characterization of WS_2 residues

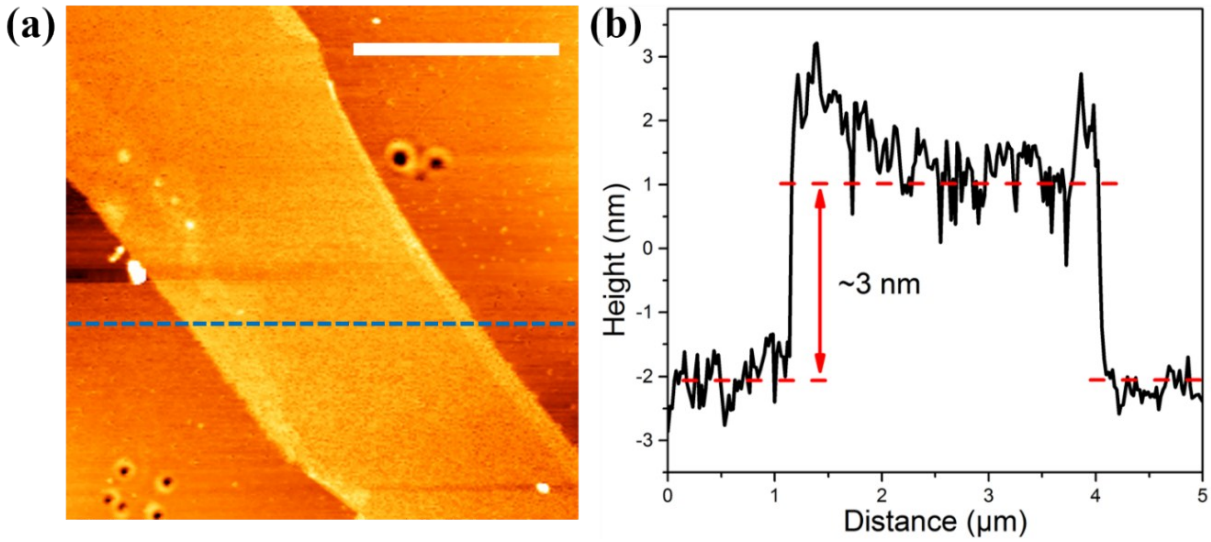

Figure S1. (a) AFM topological mapping of the WS_2 residues on SiO_2/Si after being in contact with DI water. Scale bar: 2μm. (b) Corresponding line profile for the blue dashed line in (a).

Figure S1(a) presents an AFM topological map of the WS_2 residues on SiO_2/Si after transferring a layer of h-BN using the standard wet transfer method. The line profile (Figure S1(b)) for the blue dashed line in Figure S1(a) shows that the thickness of the surviving WS_2 is ~3nm after standard wet transfer, indicating the material left on the surface is multilayer WS_2.

S2. Detection of WO_3 or W-oxide formation

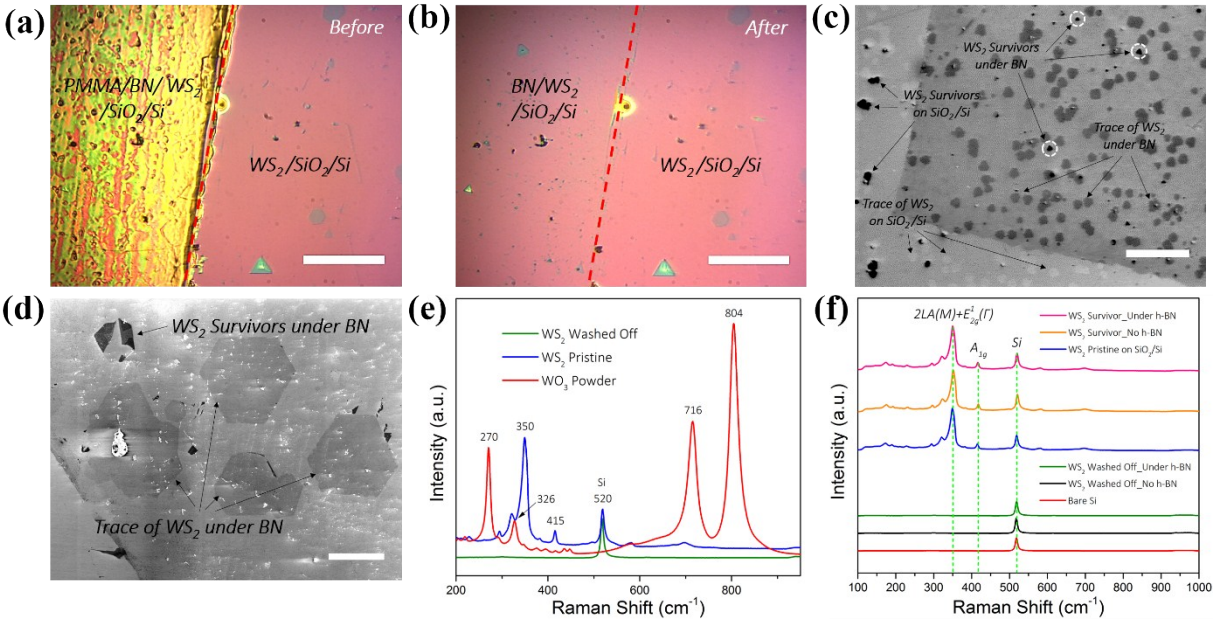

Figure S2. Probing WO_3 or W-oxide formation after transferring a layer of h-BN onto as-grown WS_2 using the standard wet transfer method. Optical images of WS_2 with a layer of h-BN on top before (a) and after (b) PMMA removal. Scale bar: 100μm. (c) SEM image of the trace of the WS_2 crystals on SiO_2/Si with and without h-BN on top. Scale bar: 0.5mm. (d) Zoomed-in SEM image of the trace of surviving WS_2 and surviving WS_2 under h-BN. Scale bar: 50μm. (e) Raman spectra of washed off WS_2, pristine WS_2 and WO_3 powder measured using 532nm excitation. (f) Comparison of Raman spectra among pristine WS_2 on SiO_2/Si, surviving WS_2 with and without h-BN on top after exposure to water, bare Si, washed off WS_2 with and without h-BN on top.

Figure S2(a) shows the optical image of WS_2 with a PMMA/h-BN stack on top. After soaking in acetone at 45^{o}C for 2 hours to remove PMMA, as shown in Figure S2(b), it was found that PMMA, which sits on top of h-BN, can be well removed during this process and the WS_2 will not be removed from the substrate by the acetone. The small optical contrast from the h-BN film on SiO_2 is attributed to its negligible opacity in the visible spectrum arising from its large band gap (>5 eV), making it hard to detect. The high transparency of the h-BN makes it easy to find WS_2 survivors and the traces of WS_2 crystals using an optical microscope even when it is covered with a layer of h-BN film. According to the optical images, it seems that there is still some residue of the material lying at locations where the WS_2 triangles or hexagons used to be before exposure to DI water. If WS_2 has been changed to some other material, which has a large band gap, it might be transparent under optical microscope. So it is necessary to examine the samples under SEM to see whether there is anything left on the surface. From the SEM images as shown in Figures S2(c) and (d), it was confirmed that just a very small number of WS_2 domains were left on the surface after transferring a layer of h-BN using the standard wet transfer method. The trace of WS_2 under h-BN on top (darker in contrast) and without h-BN (brighter in contrast) can be easily found in Figure S2(c). The water might be oxidizing the WS_2 and changing it to WO_3 or other W-oxides during the transfer process. So it is necessary to check the darker and brighter areas using Raman spectroscopy in order to confirm whether the disappearance of WS_2 leads to a rise of 2D W-oxides.

It was reported by Xu et al.[1] that Raman peaks centered at 272, 326, 717 and 807 cm^{-1} can be found from WO_3, the first two are induced by W-O-W bending mode vibration and the other two correspond to W-O-W stretching vibration mode. As can be seen in Figure S2(e), peaks in the Raman spectrum at similar positions (270, 326, 716 and 804 cm^{-1}) were found for

pure WO_3 powder deposited onto the sample for the measurement, which is the same as the precursor used to grow monolayer WS_2 by CVD. There is no difference between the spectra of washed off WS_2 without h-BN on top and bare Si, indicating that the WS_2 was completely washed off and no W-oxides were left on the surface after exposure to water. The Raman spectra of pristine WS_2 on SiO_2/Si, surviving WS_2 with and without h-BN on top after exposure to DI water were compared and show almost the same peak positions, but with slightly different peak intensity. Although the contrast for washed off WS_2 under SEM is brighter on SiO_2/Si and darker under h-BN, as can be seen from Figure S2(c), that their Raman spectra are almost the same (Figure S2(f)), showing only one peak centered at 520 cm^{-1}, which corresponds to bare Si. The contrast in both SEM and optical microscopy can be attributed to the concave surface left by the detachment of WS_2, most likely formed during the initial growth of WS_2 on the SiO_2 surface by CVD at high temperatures.

S3. Characterization of CVD-grown multilayer h-BN

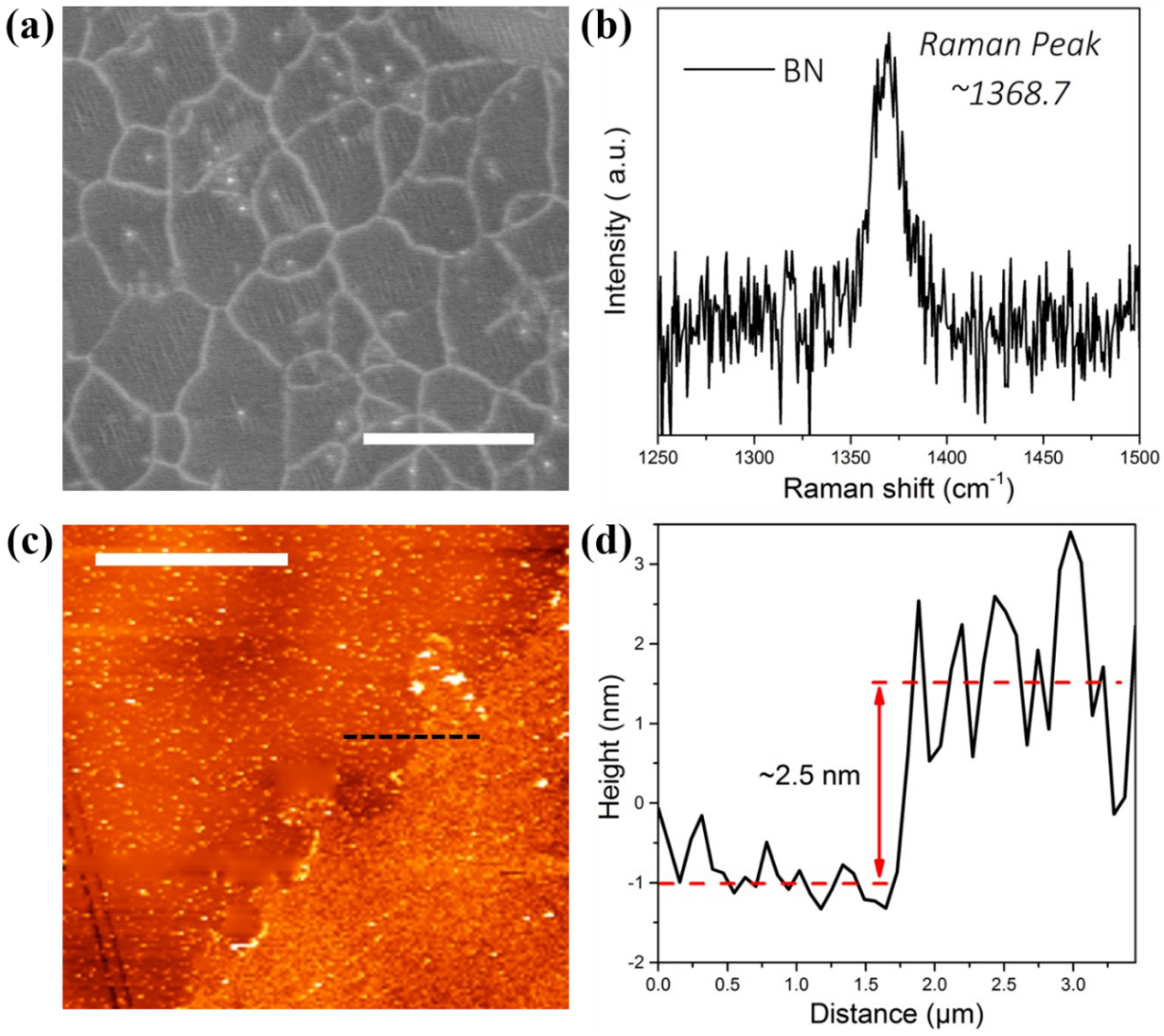

Figure S3. (a) A typical SEM image of the CVD-grown multilayer h-BN film on Cu substrate. Scale bar: 10μm. (b) Raman spectrum of the transferred h-BN film on SiO_2/Si substrate. (c) AFM topological mapping of the transferred h-BN film. Scale bar: 5μm. (d) Corresponding height profile taken across the black dashed line in (c).

Figure S3(a) presents a typical SEM image of the CVD-grown continuous h-BN film on Cu. The Raman spectrum, as can be seen from Figure S3(b), shows a characteristic peak centered at ~1368.7 cm^{-1}, which indicates the film thickness to be multilayer. Figures S3(c)

and (d) gives a typical AFM measurement, showing the thickness of the h-BN film is ~2.5nm following transfer onto a SiO_2/Si substrate.

S4. Characterization of CVD graphene

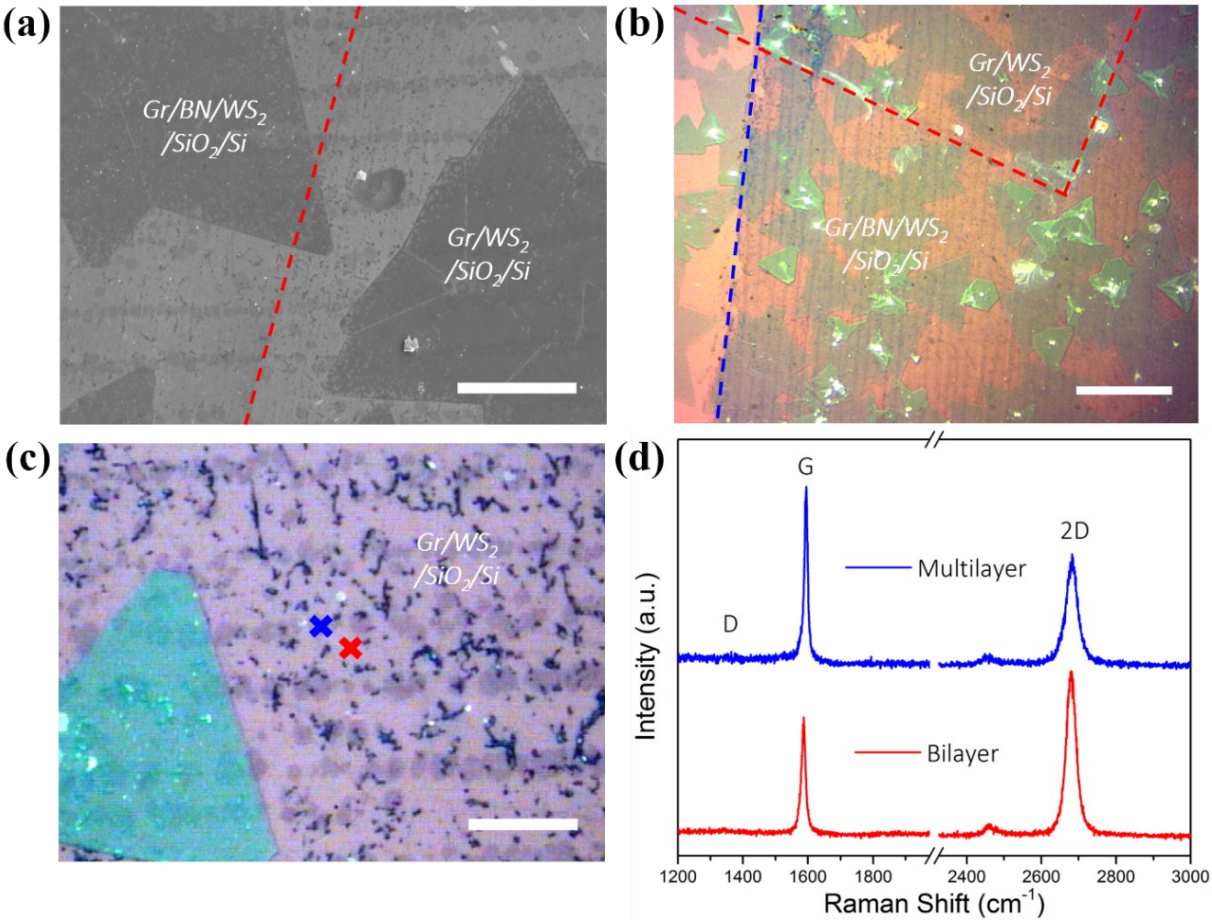

Figure S4. (a) SEM image of graphene/h-BN/WS_2 (left part) and graphene/WS_2 (right part) on SiO_2/Si. Scale bar: 50μm. (b) Optical image of the graphene/h-BN/WS_2 stack on SiO_2/Si. The blue dashed line and the red dashed line indicate the boundary of graphene and h-BN film, respectively. Scale bar: 200μm. (c) Optical image of the graphene/WS_2 stack. Scale bar: 30μm. (d) Raman spectra of the marked spots with corresponding colored crosses showing the existence of bi- and multi-layer graphene. Blue line: multilayer graphene. Red line: bilayer graphene.

Figures S4(a) and (b) present typical areas of the graphene/h-BN/WS_2 stack on SiO_2/Si examined by SEM and optical microscopy, respectively. The non-uniform contrast indicates the variation of the film thickness.[2] The graphene film is continuous with several thicker graphene strips. Figure S4(d) shows the Raman spectra of two marked spots with different color in Figure S4(c). The 2D/G intensity ratio of the spectra in red is ~1.3, which indicates bilayer graphene.[3–6] The blue spectrum with a ratio of ~0.6 indicates that the graphene is about 2-4 layers thick.[7] The D peak (~1350 cm^{-1}) used to identify the level of defects[8] in graphene was found to be negligible for both spectra, indicating the high quality of the transferred CVD graphene.

Reference

(1) Xu, L.; Yin, M.; Liu, S. F. Agx@WO3 Core-Shell Nanostructure for LSP Enhanced Chemical Sensors. *Sci. Rep.* **2014**, *4*, 6745.

(2) Sheng, Y.; Rong, Y.; He, Z.; Fan, Y.; Warner, J. H. Uniformity of Large-Area Bilayer Graphene Grown by Chemical Vapor Deposition. *Nanotechnology* **2015**, *26*, 395601.

(3) Liu, L.; Zhou, H.; Cheng, R.; Yu, W. J.; Liu, Y.; Chen, Y.; Shaw, J.; Zhong, X.; Huang, Y.; Duan, X. High-Yield Chemical Vapor Deposition Growth of High-Quality Large-Area AB-Stacked Bilayer Graphene. *ACS Nano* **2012**, *6*, 8241–8249.

(4) Luo, Z.; Yu, T.; Shang, J.; Wang, Y.; Lim, S.; Liu, L.; Gurzadyan, G. G.; Shen, Z.; Lin, J. Large-Scale Synthesis of Bi-Layer Graphene in Strongly Coupled Stacking Order. *Adv. Funct. Mater.* **2011**, *21*, 911–917.

(5) Li, X.; Cai, W.; An, J.; Kim, S.; Nah, J.; Yang, D.; Piner, R.; Velamakanni, A.; Jung, I.; Tutuc, E.; *et al.* Large-Area Synthesis of High-Quality and Uniform Graphene Films on Copper Foils. *Science* **2009**, *324*, 1312–1314.

(6) Reina, A.; Jia, X.; Ho, J.; Nezich, D.; Son, H.; Bulovic, V.; Dresselhaus, M. S.; Kong, J. Large Area, Few-Layer Graphene Films on Arbitrary Substrates by Chemical Vapor Deposition. *Nano Lett.* **2009**, *9*, 30–35.

(7) Lui, C. H.; Li, Z.; Chen, Z.; Klimov, P. V; Brus, L. E.; Heinz, T. F. Imaging Stacking Order in Few-Layer Graphene. *Nano Lett.* **2010**, *11*, 164–169.

(8) Ferrari, A. C.; Meyer, J. C.; Scardaci, V.; Casiraghi, C.; Lazzeri, M.; Mauri, F.; Piscanec, S.; Jiang, D.; Novoselov, K. S.; Roth, S.; *et al.* Raman Spectrum of Graphene and Graphene Layers. *Phys. Rev. Lett.* **2006**, *97*, 187401.